

Characterization of nickel doped $\text{Zn}_7\text{Sb}_2\text{O}_{12}$ spinel phase using Rietveld refinement

L. Gama

Laboratório de Cerâmica, Departamento de Engenharia de Materiais, Centro de Ciências e Tecnologia—Universidade Federal da Paraíba, Campina Grande-PB, Brazil

C. O. Paiva-Santos^{a)}

Laboratório Computacional de Análises Cristalográficas e Cristalinas, Instituto de Química—Universidade Estadual Paulista, Araraquara SP, Brazil

C. Vila, P. N. Lisboa-Filho, and E. Longo

Laboratório Interdisciplinar de Eletroquímica e Cerâmica, Departamento de Química, Centro Multidisciplinar para o Desenvolvimento de Materiais Cerâmicos, Universidade Federal de São Carlos, São Carlos SP, Brazil

(Received 7 October 2001; accepted 6 March 2003)

$\text{Zn}_7\text{Sb}_2\text{O}_{12}$ is known to adopt an inverse spinel crystal structure, in which Zn^{2+} occupies the eight tetrahedral positions and Sb^{5+} and Zn^{2+} randomly occupy the 16 octahedral positions. Samples of $\text{Zn}_{7-x}\text{Ni}_x\text{Sb}_2\text{O}_{12}$ ($x=0, 1, 2, 3,$ and 4) were synthesized using a modified polymeric precursor method, known as the Pechini method. The crystal structure of the powders was characterized by Rietveld refinement with X-ray diffraction data. The results show that for $x=0, 1,$ and 2 Ni substitutes for Zn^{2+} in the octahedral sites, and that for $x=3$ and 4 it is assumed that Ni^{2+} replaces Zn^{2+} ions in both the octahedral and tetrahedral positions. It is also observed for $x=3$ and 4 the formation of two spinel phases. © 2003 International Centre for Diffraction Data.

[DOI: 10.1154/1.1572486]

Key words: spinel structure, X-ray diffraction, Rietveld method, Pechini method

INTRODUCTION

The zinc-antimony spinel $\text{Zn}_7\text{Sb}_2\text{O}_{12}$, has been studied because of its large variety of industrial and technological applications, from ceramic pigments to voltage ceramic varistors (Ezhilvalavan and Kutty, 1996; Poleti *et al.*, 1994). When doped with magnetic ions, e.g., nickel and cobalt, this system has considerable potential in magnetic storage technology (Schiessl *et al.*, 1996). In particular, the system $\text{Zn}_{7-x}\text{Ni}_x\text{Sb}_2\text{O}_{12}$ ($x=3$ and 4) possesses magnetic irreversibility and is considered an excellent candidate to be catalogued as a spin-glass (Lisboa-Filho *et al.*, 2000).

This spinel structure accommodates a large number of different cations, occupying two possible different crystallographic sites: octahedral or tetrahedral. Some inorganic compounds with the spinel structure display significant cation disorder (Sickafus *et al.*, 1999). Figure 1 presents the spinel unit cell. In order to study Ni-doped $\text{Zn}_7\text{Sb}_2\text{O}_{12}$, polycrystalline samples were synthesized using a modified polymeric precursor method, known as the Pechini method (Pechini, 1967). The resulting phases and crystal structures were characterized using X-ray powder diffraction (XRPD) and the Rietveld refinement method (Rietveld, 1969).

In terms of crystal structure, for a complete study of the physical properties of the spinel Ni-doped structure, it is necessary to introduce the parameter u that describes the oxygen position (u, u, u) in the unit cell. This parameter indicates the deviations in the anionic sublattice and varies according to the cation size variations in the structure. The knowledge of u is crucial to understanding the origin of possible magnetic

interactions between the AA, BB, and AB sites of the spinel structure AB_2O_4 . The existence and strength of exchange interactions are fully dependent on the metal ion–oxygen–metal ion angle.

This paper reports part of an extensive project to fully characterize the $\text{Zn}_7\text{Sb}_2\text{O}_{12}$ structure and its derived doped phases. In a previous study (Lisboa-Filho *et al.*, 2000), it was reported from infrared spectroscopy analysis that Ni probably occupies the tetrahedral $8a$ site for $x \geq 2$. Rietveld re-

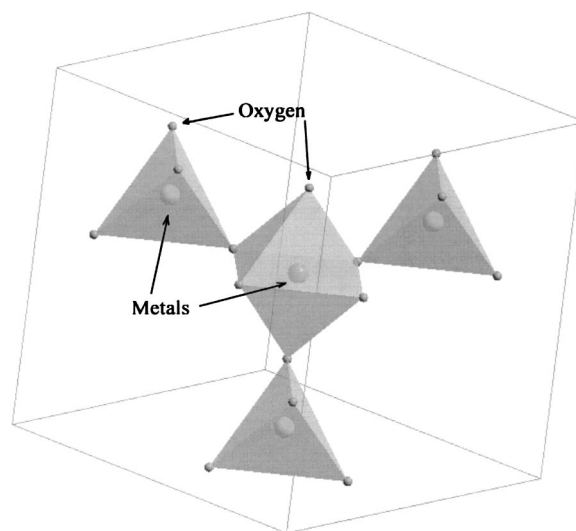


Figure 1. Spinel unit cell showing an octahedra surrounded by tetrahedra. Large circles correspond to the oxygen ions, small open circles are the metallic ions at tetrahedral sites and small dark circles represent metallic ions at octahedral sites.

^{a)} Author to whom correspondence should be addressed; electronic mail: copsanto@iq.unesp.br

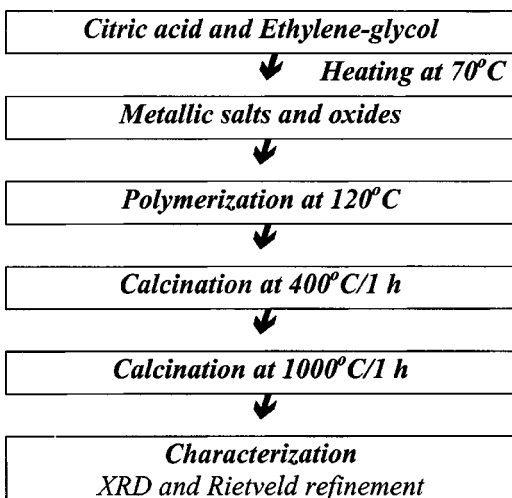


Figure 2. Flow chart for the synthesis of $Zn_{7-x}Ni_xSb_2O_{12}$ powders.

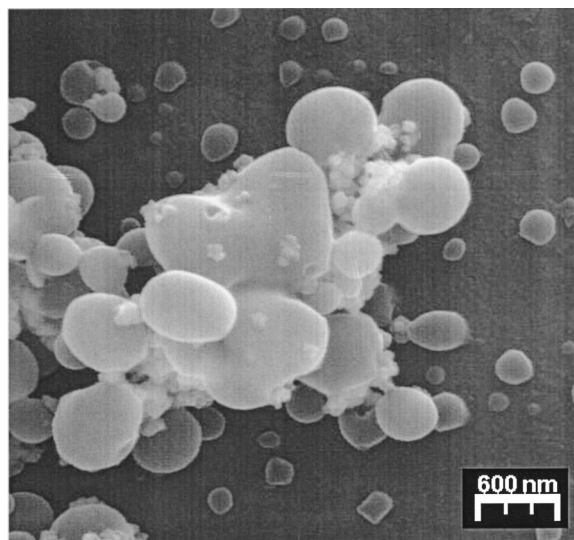


Figure 3. SEM micrograph for $Zn_3Ni_4Sb_2O_{12}$.

finements were then carried out to corroborate this IR analysis, and to understand the ferromagnetic behavior described by Lisboa-Filho *et al.* (2000).

EXPERIMENTAL PROCEDURE

Synthesis

The $Zn_{7-x}Ni_xSb_2O_{12}$ polycrystalline samples were synthesized using a chemical route based on the Pechini method following the procedure shown in Figure 2. Mixed metal citrate solutions were prepared with a citric acid/metal ratio of 1/3 (molar basis). The solution was homogenized by magnetic stirring at 70 °C, and then ethylene glycol was added to this solution to obtain a citric acid/ethylene glycol ratio of 60/40 by mass. Polymerization occurred at 120 °C, after which the resin was calcined at 400 °C in order to eliminate any organic material. After that, in order to obtain a better crystalline phase, the powder was calcined at 1000 °C for 1 hour.

Crystallographic characterization

The X-ray diffraction data were obtained using a Siemens D5000 diffractometer in the range $20^\circ \leq 2\theta \leq 110^\circ$, with copper radiation monochromated by graphite crystal in the diffracted beam ($\lambda k\alpha_1 = 1.5406$, $\alpha_2 = 1.5444$ Å, ratio $k\alpha_2/k\alpha_1 = 0.500$), 40 kV, 30 mA, divergence slit = 1°, step time = 12 s, step size = 0.02°, and scintillation detector.

The program DBWS9807a (Young *et al.*, 1999), which is an upgraded version of DBWS-9411 described by Young *et al.* (1995), was used for the Rietveld refinements. The pseudo-Voigt function (Young and Wiles, 1982), defined as

$$\phi = [\eta L + (1 - \eta)G],$$

where L is the Lorentz function, G is the Gauss function, and η is the mixing parameter representing the fraction of Lorentzian content, was used to fit the peak profiles.

The ideal cubic crystal structure of spinel (space group $Fd\bar{3}m$, origin at center $3m$) was taken as the initial model (Sawada, 1995). The tetrahedrally coordinated cations (Zn^{2+}) are at site $8a$ (1/8, 1/8, 1/8), the octahedrally coordi-

nated cations (Ni^{2+} , Zn^{2+} , and Sb^{5+}) are at site $16d$ ($\frac{1}{2}, \frac{1}{2}, \frac{1}{2}$), and the oxygen atoms are at the special position $32e$ (u, u, u), where u is a refinable parameter. The DM-PLOT (Marciniak, 1997) Rietveld difference plot program was used to monitor the refinements.

The following parameters were refined: sample displacement, unit cell parameter, oxygen position u , isotropic atom displacement B , FWHM, the mixing parameter η , and scale factor. The background was fitted by third degree polynomial. Furthermore, to better determine the spinel phase stoichiometry, the Zn and Ni occupation parameters were refined and constrained to have their sum equal to 1.0, with the same atomic displacement for Zn and Ni.

During the refinements for $Zn_4Ni_3Sb_2O_{12}$ and $Zn_3Ni_4Sb_2O_{12}$, η reached values greater than 1, and satellite points were observed around the maxima of the peaks in the Rietveld difference plots. According to Young and Sakhthivel (1988), these features may be because of a bimodal distribution of crystallite size. For these two phases, the two different crystallite sizes were modeling by treating the material as a two phase mixture, each having the same crystal structure but different FWHM. Figure 3 is an SEM micrograph of the $Zn_3Ni_4Sb_2O_{12}$ powder in which one can observe the bimodal distribution of crystallite size.

For all Ni doped samples it was assumed that the Ni^{2+} and Zn^{2+} share the octahedral site. Concerning the tetrahedral sites, it was considered that $Zn_6Ni_1Sb_2O_{12}$ and $Zn_5Ni_2Sb_2O_{12}$ have only Zn at this site. On the other hand, for $Zn_3Ni_4Sb_2O_{12}$, Zn and Ni share the tetrahedral site. For $Zn_4Ni_3Sb_2O_{12}$, the refinement of Zn and Ni occupancies at this site did not converge; it was then considered to have the $8a$ site filled with Zn, although the bimodal distribution of crystallite size can be considered an indication of possible differences in the occupancies, as was proposed for the case with $x = 4$.

Unit cell parameters and the oxygen positional parameter u for each spinel phase were also studied. For $x > 2$ a small amount of NiO phase was observed.

TABLE I. Rietveld refinement results for the $Zn_{7-x}Ni_xSb_2O_{12}$ samples. The refinement indexes R_p , R_{wp} , R_{exp} , R_{Bragg} and the goodness of fit S are defined by Young and Wiles (1982). Phase 1 means the phase with smaller crystallite size and phase 2 means the phase with bigger crystallite size. (e.s.d.'s are given in parentheses.)

	$Zn_{7-x}Ni_xSb_2O_{12}$ spinel				
	$x=0$	$x=1.0$	$x=2.0$	$x=3.0$	$x=4.0$
R_{wp}	10.38	10.21	9.89	11.77	11.35
R_{exp}	10.00	9.68	9.51	10.62	10.05
S	1.04	1.05	1.04	1.11	1.12
R_{Bragg}	6.37	4.18	10.73	5.30	3.88
				2.52	3.40
	Spinel phases				
a (Å)	8.6010(3)	8.5804(3)	8.5589(4)	8.5412(4) ^a	8.5169(6) ^a
				8.5419(2) ^b	8.5192(3) ^b
u	0.2569(8)	0.2578(8)	0.2610(9)	0.263(2) ^a	0.262(2) ^a
				0.256(1) ^b	0.257(2) ^b

^aPhase 1.

^bPhase 2.

RESULTS AND DISCUSSION

The refinement results are summarized in Table I, Table II, and Figures 4 and 5. These two figures give the Rietveld plots for the cases with $x=0$ and $x=4$, respectively. Some of the following discussion requires values for the ionic radii of the cations, with coordination numbers (CN) IV and VI. For CN=IV: $Ni^{2+}=0.55$ Å, $Zn^{2+}=0.60$ Å. For CN=VI: $Ni^{2+}=0.69$ Å, $Zn^{2+}=0.74$, and $Sb^{5+}=0.60$ Å (Shannon, 1976).

Lattice parameter calculations

The variation of the cell parameter a as a function of the amount of dopant added is shown in Figure 6. It is observed that a decreases linearly with the substitution of Zn^{2+} by the smaller ion Ni^{2+} . Observing the decrease in the unit cell size, one could consider that Ni substitutes for Zn at the octahedral and/or tetrahedral sites, which is in agreement with the results obtained by infrared spectroscopic analysis (Lisboa-Filho *et al.*, 2000). It is also noted that $Zn_4Ni_3Sb_2O_{12}$ and $Zn_3Ni_4Sb_2O_{12}$ provided unit cell parameters for the two different crystallite sizes that were significantly different only for $x=4$.

The correlation factor R^2 for the fit for two situations are given in Figure 6. The results show a small difference, with the better value for the case where Ni^{2+} is at the tetrahedral and octahedral sites. R^2 indicates, for both cases, that the

TABLE II. Cation distributions in the tetrahedral and octahedral sites of the spinel phase $Zn_{7-x}Ni_xSb_2O_{12}$ with $x=0, 1, 2, 3$, and 4. Results after Rietveld refinements.

Spinel phase	Ions distributions	
	Tetrahedral site	Octahedral site
$Zn_3Ni_4Sb_2O_{12}$	$Zn_{2.82(15)}Ni_{0.18(15)}$	$Zn_{0.18(15)}Ni_{3.82(15)}$
$Zn_4Ni_3Sb_2O_{12}$	Indeterminate	Indeterminate
$Zn_5Ni_2Sb_2O_{12}$	Zn_3	Zn_2Ni_2
$Zn_6Ni_1Sb_2O_{12}$	Zn_3	Zn_3Ni_1
$Zn_7Sb_2O_{12}$	Zn_3	Zn_4

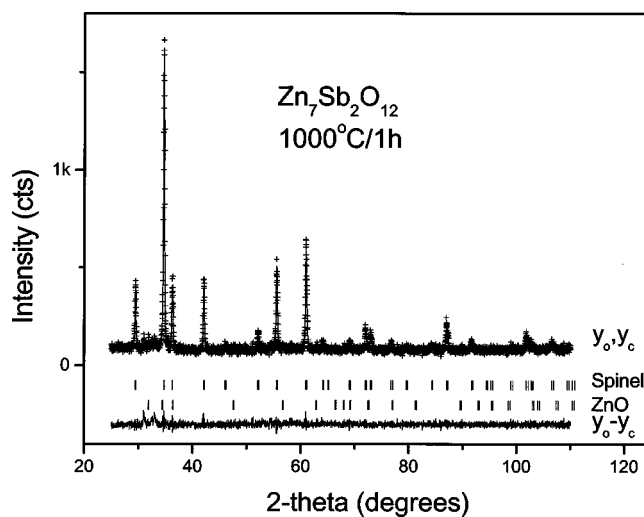


Figure 4. Rietveld plot for $Zn_7Sb_2O_{12}$.

dependence of the lattice parameter with x obeys Vegard's law (Cormack *et al.*, 1988), being sensitive to the amount of dopant added.

Nickel occupation

In order to clarify the observed differences in the phase that contains two crystallite sizes, three distinct possibilities were also tested. They are as follows.

(a) Ni^{2+} substitutes for Sb^{5+} . The larger ionic radius of Ni will increase the unit cell. This case is not probable because of the difference in the oxidation state.

(b) Not all the Zn^{2+} was removed from the octahedral site, i.e., the Zn^{2+} and Ni^{2+} are still sharing the same site.

(c) Ni^{2+} shares the tetrahedral site with Zn^{2+} .

Assuming that these two last assumptions are correct, the refinement data, summarized in Table I, were analyzed and the crystalline site distributions were calculated. The obtained results are shown in Table II.

The analysis of the FWHM, shown in Figure 7, reveals that the phase with Ni only at the octahedral site is broadened, indicating that this phase has a smaller crystallite size than the second phase.

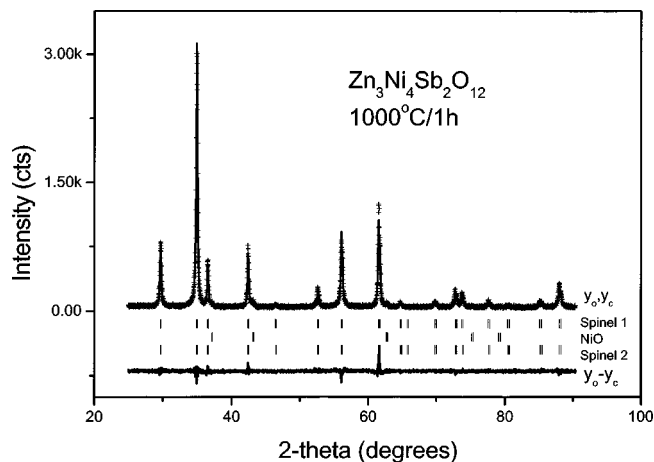


Figure 5. Rietveld plot for $Zn_3Ni_4Sb_2O_{12}$. Phase 1 means the phase with smaller crystallite size and phase 2 means the phase with bigger crystallite size.

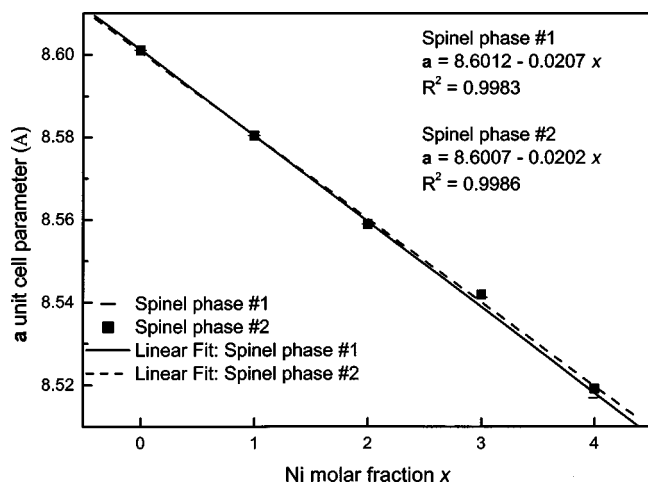


Figure 6. Unit cell variation with Ni molar fraction for $Zn_{7-x}Ni_xSb_2O_{12}$ spinel samples. The correlation factors R^2 were calculated for the cases where Ni is only at the tetrahedral site and where Ni is at the tetrahedral and octahedral sites. Phase 1 means the phase with smaller crystallite size and phase 2 means the phase with bigger crystallite size.

Oxygen-metal distance calculations

Using the unit cell parameter (a) and the oxygen position parameter (u), the distances between the oxygen-metal distances were calculated for the tetrahedral (D_t) and the octahedral sites (D_o) using the relations (Navrotsky and Kleppa, 1967)

$$D_{(t)} = a\sqrt{3}\left(u - \frac{1}{8}\right) \quad (1)$$

and

$$D_{(o)} = a\left(3u^2 - 2u + \frac{3}{8}\right)^{1/2}. \quad (2)$$

The average size distance B–O for the octahedral site decreases with nickel occupation. It is known that the nickel atoms are more likely to occupy the octahedral sites when substituting for zinc. Since Ni^{2+} is bigger than Zn^{2+} , the B–O distances in the octahedral sites decrease as the value of x increases. Complete occupation of the octahedral sites

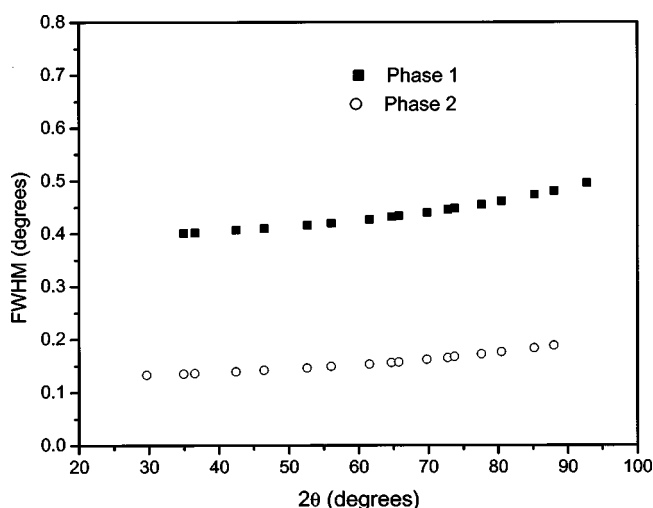


Figure 7. Full-width at half-maximum of the two spinel phases for $x=4$. Phase 1 means the phase with smaller crystallite size and phase 2 means the phase with bigger crystallite size.

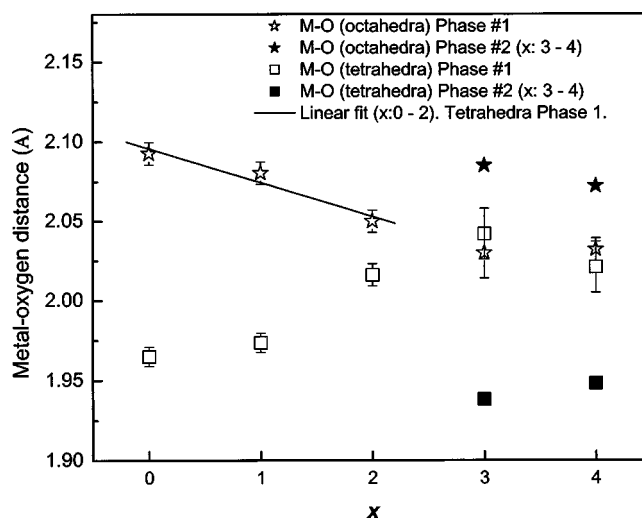


Figure 8. Interatomic metal–oxygen distances in the tetrahedra and octahedra for the spinel phase $Zn_{7-x}Ni_xSb_2O_{12}$, $x=0, 1, 2, 3$, and 4 . Phase 1 means the phase with smaller crystallite size and phase 2 means the phase with bigger crystallite size.

by Ni^{2+} occurs for values of $x > 3$; after that the nickel atoms start replacing zinc at the tetrahedral sites.

On the other hand, the average A–O distance increases up to $x > 3$, and after that it also decreases. The variations in the metal–oxygen (A–O) interatomic distance in the tetrahedral (D_t) and in the octahedral (D_o) sites can be seen in Figure 8. The calculated values, $D_{t(Zn-O)} = 0.1965$ nm and $D_{o(Zn-O)} = 0.2093$ nm for $x=0$, are close to those reported in the literature (Poix, 1965), $D_{t(Zn-O)} = 0.1927$ nm and $D_{o(Zn-O)} = 0.2100$ nm.

It also can be noted that the distance B–O in the octahedral sites decreases and the distance A–O in the tetrahedral increases with dopant addition, up to $x=2$. Otherwise, for $x=3$ and 4 , where two crystallite sizes were present, the results showed that for the component with the smaller crystallite size, the distances D_o and D_t did not vary within one standard deviation. This is an indication that the ratio Ni/Zn reached its maximum value.

For the phase with bigger crystallite size, Ni^{2+} also occupies the tetrahedral site, substituting for Zn^{2+} , which causes a decrease of the A–O distance in the tetrahedral site. According to the results presented here, it is possible to conclude that for $0 < x \leq 2$ Ni^{2+} occupies the $16d$ site and substitutes for Zn^{2+} . Furthermore, for $x \geq 3$ Ni^{2+} substitutes for Zn^{2+} in both $16d$ and $8a$ sites.

CONCLUSIONS

Rietveld refinement analyses of powder X-ray diffraction (XRD) measurements indicated that for $x \leq 2$ the Ni occupies the octahedral sites, substituting for Zn. For $x \geq 3$ the Ni occupies the octahedral and the tetrahedral sites, again substituting for the zinc ion.

The crystallite size of the phase with Ni at both sites appears to substantially exceed the crystallite size of the phase with Ni only in the octahedral site.

ACKNOWLEDGMENTS

The authors acknowledge the financial support of the Brazilian funding agencies FAPESP, CNPq, and CAPES.

- Cormack, A. N., Lewis, G. V., Parker, S. C., and Catlow, C. R. A. (1988). "On the cation distribution of spinels," *J. Phys. Chem. Solids* **49**, 53–57.
- Ezhilvalavan, S., and Kutty, T. R. N. (1996). "Low voltage varistors based on zinc antimony spinel $Zn_7Sb_2O_{12}$," *Appl. Phys. Lett.* **68**, 2693.
- Lisboa-Filho, P. N., Gama, L., Paiva-Santos, C. O., Varela, J. A., Ortiz, W. A., and Longo, E. (2000). "Crystallographic and magnetic structure of polycrystalline $Zn_{7-x}Ni_xSb_2O_{12}$ spinels," *Mater. Chem. Phys.* **65**, 208–211.
- Marciniak, H. (1997). "DMPLOT—Plot view program for Rietveld refinement method, Version 3.48."
- Navrotsky, A., and Kleppa, O. J. (1967). "Thermodynamics of cation distributions in single spinel," *J. Inorg. Nucl. Chem.* **29**, 2701–2714.
- Pechini, M. (1967). U.S. Patent No. 3,330,697–1967.
- Poix, P. (1965). "Sur une methode de determination des distances cation-oxygene dans les oxydes mixtes a structure spinelle—application des valeurs a quelques cas particuliers," *Bull. Soc. Chim. Fr.* **4**, 1085.
- Poleti, D., Vasovic, C., Karanovic, L., and Brankovic, Z. (1994). "Synthesis and characterization of ternary Zinc–Antimony–Transition metal spinels," *J. Solid State Chem.* **112**, 39–44.
- Rietveld, H. M. (1969). "A profile refinement method for nuclear and magnetic structures," *J. Appl. Crystallogr.* **2**, 65–69.
- Sawada, H. (1995). "An electron density residual study of magnesium aluminium oxide spinel," *Mater. Res. Bull.* **30**, 341–345.
- Schiessl, W., Potzel, W., Karzel, H., Steiner, M., Kalvius, G. M., Martin, A., Krause, M. K., Halevy, I., Gal, J., Schäfer, W., Will, G., Hillberg, M., and Wäppling, R. (1996). "Magnetic properties of $ZnFe_2O_4$ spinel," *Phys. Rev. B* **53**, 9143–9152.
- Shannon, R. D. (1976). "Revised effective ionic radii and systematic studies of interatomic distances in halides and chalcogenides," *Acta Crystallogr., Sect. A: Cryst. Phys., Diffr., Theor. Gen. Crystallogr.* **A32**, 751–767.
- Sickafus, K. E., Wills, J. M., and Grimes, N. W. (1999). "Structure of spinel," *J. Am. Ceram. Soc.* **82**, 3279–3292.
- Young, R. A., Larson, A. C., and Paiva-Santos, C. O. (1999). "User's guide to program DBWS-9807a for Rietveld analysis of X-Ray and neutron powder diffraction patterns with a PC and various other computers," School of Physics Georgia Institute of Technology Atlanta, GA, 1999.
- Young, R. A., and Sakhivel, A. (1988). "Bimodal distributions of profile-broadening effects in Rietveld refinement," *J. Appl. Crystallogr.* **21**, 416–425.
- Young, R. A., Sakhivel, A., Moss, T. S., and Paiva-Santos, C. O. (1995). "DBWS-9411, an upgrade of the DBWS*.* programs for Rietveld refinement with PC and mainframe computers," *J. Appl. Crystallogr.* **28**, 366–367.
- Young, R. A., and Wiles, D. B. (1982). "Profile shape functions in Rietveld refinements," *J. Appl. Crystallogr.* **15**, 430–438.